Stem Cell Reports
Article

ISSCR

OPEN ACCESS

Tissue origin of cytotoxic natural killer cells dictates their differential roles in mouse digit tip regeneration and progenitor cell survival

Nadjib Dastagir,[1,2,3] Zachery Beal,[1] and James Godwin[1,2,*]
[1]The Jackson Laboratory, Bar Harbor, ME 04609, USA
[2]Mount Desert Island Biological Laboratory, Kathryn W. Davis Center for Regenerative Biology and Aging, Salisbury Cove, ME 04609, USA
[3]Medical School of Hanover, 30659 Hannover, Germany
*Correspondence: james.godwin@jax.org
https://doi.org/10.1016/j.stemcr.2022.01.006

SUMMARY

Regeneration of amputated digit tips relies on mesenchymal progenitor cells and their differentiation into replacement bone and tissue stroma. Natural killer (NK) cells have well-characterized roles in antigen-independent killing of virally infected, pre-tumorous, or stressed cells; however, the potential for cytotoxic activity against regenerative progenitor cells is unclear. We identified NK cell recruitment to the regenerating digit tip, and NK cytotoxicity was observed against osteoclast and osteoblast progenitors. Adoptive cell transplants of spleen NK (SpNK) or thymus NK (ThNK) donor cells into immunodeficient mice demonstrated ThNK cell-induced apoptosis with a reduction in osteoclasts, osteoblasts, and proliferative cells, resulting in inhibition of regeneration. Adoptive transfer of NK cells deficient in NK cell activation genes identified that promotion of regeneration by SpNK cells requires *Ncr1*, whereas inhibition by ThNK cells is mediated via *Klrk1* and perforin. Successful future therapies aimed at enhancing regeneration will require a deeper understanding of progenitor cell protection from NK cell cytotoxicity.

INTRODUCTION

Unlocking latent regeneration in mammals or developing future regenerative therapies will rely on understanding factors regulating successful regeneration in model systems. Humans and mice have analogous regeneration potential after amputation in terminal phalangeal element (P3) digit tips (Storer and Miller, 2020). This involves a wound healing response characterized by immune cell recruitment, epithelial closure, and a primary bone catalytic step performed by bone-degrading osteoclasts. When the P3 bone is degraded, several sources of stem cell-like progenitors are recruited to the wound (Lehoczky and Tabin, 2015; Storer et al., 2020; Rinkevich et al., 2011), some of which differentiate to form bone-producing osteoblast cells and the mesenchymal tissues that will regenerate the missing tissue, including ossified bone. The digit tip regeneration process is distinct from fracture healing; it occurs without using a chondrocyte intermediate (Dawson et al., 2016). Understanding digit tip regeneration will provide important insights into stem cell-mediated repair and regeneration in a range of contexts.

The immune system is a major regulator of fracture healing but has been poorly studied in epimorphic regeneration models such as the mouse digit tip. Macrophages are innate immune cells critical for success of digit tip regeneration in mice and limb regeneration in salamanders (Godwin et al., 2013; Simkin et al., 2017). Macrophage-monocyte progenitors differentiate into osteoclasts, cells required for remodeling of fractures and initiation of the catabolic phase of digit tip regeneration. Natural killer (NK) cells are another type of innate immune cells of the lymphoid lineage that are recruited to injury sites (Liippo et al., 2010) The main function of NK cells is to recognize foreign or virally infected cells or cells that have altered metabolism (i.e., cancer cells) and induce apoptosis or cell lysis (Backes et al., 2018). Little is known about NK cell activity in regeneration, fracture healing, or even wound healing *in vivo*. NK cells may play a role in removal of damaged cells located at the site of injury (Tosello-Trampont et al., 2017); however, cytotoxicity is governed by a set of receptors (including NKP46 and NKG2D) and the ratio and distribution of activating or inhibitory ligands on that target cell membrane (Vivier et al., 2008). Activated cytotoxic NK cells kill by delivering lytic granules or death-inducing cytokine secretion (Fauriat et al., 2010). In some circumstances, this activity can be directed against other immune cells (T cells or macrophages) (Liippo et al., 2010); however, it is not known whether significant cytotoxicity is mediated against progenitor cells important for wound repair and regeneration *in vivo*.

The exact role of NK cells in repair and regeneration is unclear. In fracture healing and inflammatory bone diseases, NK cells promote mesenchymal stem cell (MSC) recruitment and osteoclastogenesis (Almeida et al., 2016; Soderstrom et al., 2010). Advances in NK cell biology have identified new NK lineages with distinct origins and developmental pathways (Sojka et al., 2014), but the potential for NK cell destruction in repair or regeneration has not been evaluated. We tested the function of NK cells from two divergent NK lineages for their role in regeneration. NK cells from splenic or thymic reserves

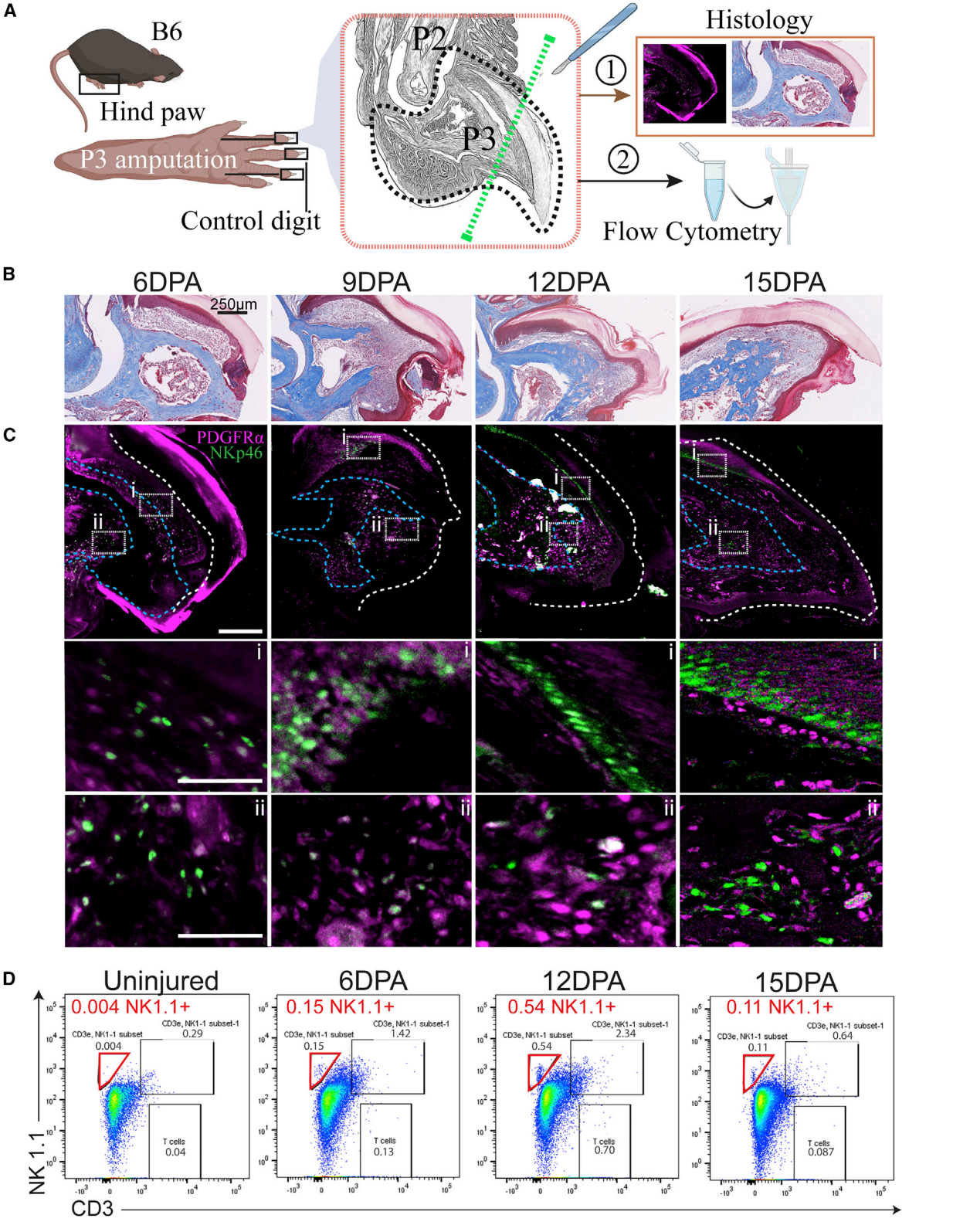

(legend on next page)

can migrate into regenerating digits and regulate several phases of the repair process. Although splenic NK (SpNK) cells promote regeneration via an NKP46 (Ncr1)-mediated genetic pathway, thymus-derived NK (ThNK) cells inhibit regeneration through NKG2D (Klrk1)- and perforin (Prf1)-mediated mechanisms. ThNK cells are more cytotoxic than SpNK cells against osteoclast and osteoblast progenitors in *ex vivo* assays. *In vivo*, SpNK cells promote proliferation, osteoblast accumulation, and differentiation without cytotoxicity, whereas ThNK cells promote apoptosis and depletion of osteoblasts/osteoclasts required for normal regeneration. Adoptive transfer of NK cells deficient in the cytotoxicity genes Klrk1, Ncr1, or Prf1 revealed regeneration phase-specific functions in destruction of progenitor cells. NK cells have the potential to kill progenitor cells *in vivo* and regulate the repair and regeneration process.

RESULTS

NK cells are recruited to the injury site after amputation

P3-level amputations in mice, removing the distal third of the P3 bone, leaving the nail bed undamaged, result in complete regeneration of the missing tissue (Seifert and Muneoka, 2018) through predictable stages. NKP46 expression is highly restricted to NK cells in mouse and human (Vivier et al., 2008). Recruitment of NKP46$^+$ NK cells is observed by 6 days post amputation (DPA) and 9 DPA, associated with the proximal nail bed (Figure 1C). By 12 DPA, NKP46$^+$ NK cells were associated with the distal nail bed and the newly forming bone region in the proximal blastema. By 15 DPA, NK cells were less abundant but associated with the distal tip and marrow cavity (Figure 1C). In parallel, staining of PDGFRα^+ cells, labeling MSC progenitors (Storer et al., 2020) that will contribute to bone-forming osteoblast cells, was performed. PDGFRα^+ cells are concentrated under the distal nail region at 6 DPA, move down into the region surrounding the catabolized P3 bone by 9 DPA, and can be found in the undifferentiated distal tip at 12 DPA and 15 DPA (Figure 1C). To quantify NK cells over the regeneration process, we used flow cytometry (FC) (Figures 1A and 1D), capturing the early pre-catabolism phase 6 DPA, post-catabolism phase (transition to bone anabolism) 12 DPA, and terminal outgrowth phase 15 DPA. NK cell invasion of the wound peaked at the 12 DPA time point (Figure 1D).

Genetic ablation of NKP46$^+$ NK cells disrupts digit tip regeneration

We then tested the functional role of NK cells in regeneration by using a mouse model that specifically sensitizes NKP46$^+$ NK cells to diphtheria toxin (DT)-mediated cell ablation (Figure 2A; Haspeslagh et al., 2018). DT-treated animals show dramatic reductions in NK cells in the spleen, thymus, and 8 DPA digit tips via FC, validating our DT NK cell ablation protocol (Figures 2B and 2C). Micro-computed tomography (μCT) imaging identifies catabolic phase entry (hard tissue fraction decreases) and the blastema stage where mesenchymal progenitor cells accumulate (soft tissue fraction increases) and can report the cell differentiation phase (soft tissue replaced by new bone). In the B6 and NSG mouse strains, catabolism of hard tissue occurs up until 12 DPA, followed by a switch to bone anabolism. In NK cell-depleted animals, catabolism is delayed (Figures 2D and 2E), with a coupled delay in soft tissue (blastema) expansion (Figures 2D and 2E). Using the first derivative of these changes, the rate of anabolism and catabolism can be visualized, confirming these delays, where, at 28 DPA, NK cell-depleted digits are still undergoing active differentiation of stem cells to produce new bone (Figure 2F). These findings suggest a positive role of NK cells in P3 digit tip regeneration.

ThNK cells and SpNK cells traffic to regenerating digit tips but show alternative localization and frequency

Most studies of NK cells have focused on conventional blood-derived or SpNK cells; we compared these with the recently described but poorly characterized ThNK cell subset, which has an alternative GATA3 development pathway (Sojka et al., 2014). To test this, we used adoptive cell transfer (ACT) of SpNK or ThNK cells into immunodeficient allotolerant NSG mice (lacking lymphoid immunity). NK cells were isolated via untouched negative magnetic selection to avoid antibody activation (Figure S1).

Figure 1. P3-level digit tip amputations on C57Bl6/J mice show migration of natural killer (NK) cells to the wound site

(A) Histological depiction of mouse P2 and P3 bones. The surgery site is indicated by a green dashed line. Tissue taken for FC and histology is indicated by a black dashed line.

(B) Early time course of digit tip regeneration using trichrome staining.

(C) Representative confocal microscopy with dual staining of PDGFRα^+ (MSCs) and NKP46$^+$ (NK cell) invasion at each time point. (i) and (ii) show high magnification insets. Samples were counterstained with DAPI. White and blue dashed lines mark the nail and soft tissue and bone boundaries, respectively. n = 3; scale bars, 250 μm.

(D) Quantification of NK cell recruitment to the wound via FC. NK cells (red gate) defined as CD3-negative and NK1.1-positive peak at 12 DPA and subsequently decrease by 15 DPA. n = 20 digits, five mice/condition. DPA, days post-amputation

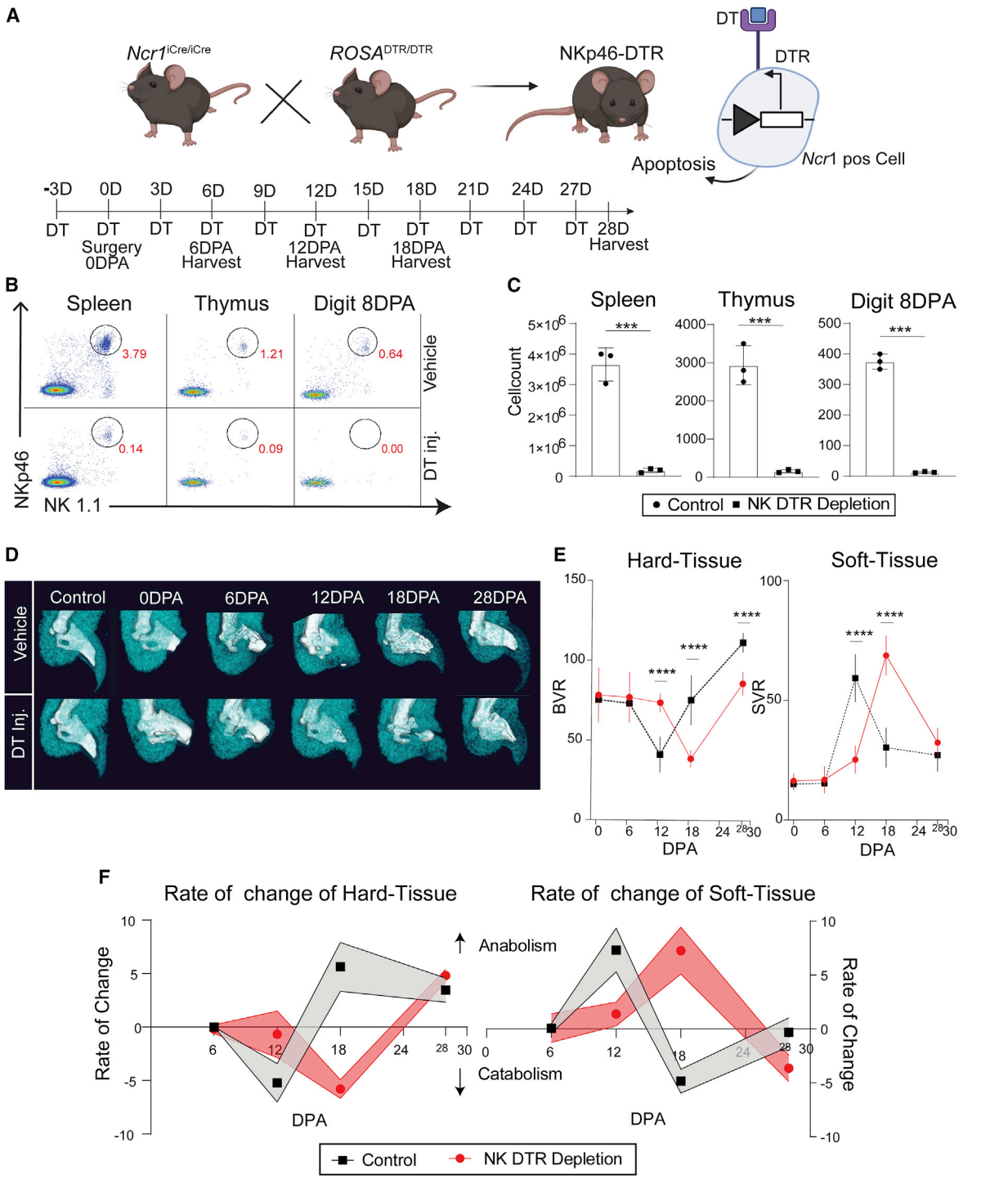

Figure 2. Systemic genetic depletion of NK cells disrupts digit tip regeneration

(A) NKP46-DT receptor (DTR) mice were created by breeding NK cell-specific Cre mice ($Ncr1^{Cre/Cre}$) with ubiquitous floxed DTR ($ROSA^{DTR/DTR}$) mice. NKP46-DTR mouse NK cells are genetically sensitized to DT, leading to apoptosis in target cells. P3-level amputations were performed 3 days after DT injection, with DT administered every 3 days until 28 DPA or harvest.

(B) Validation of NK cell depletion efficacy in the spleen, thymus, and digit tip via FC ($NKP46^+$ and $NK1.1^+$ dual-positive cells).

(C) Reduction in $NKP46^+/NK1.1^+$ dual-positive cells in DT-treated mice in all tissues tested (***$p < 0.001$, Student's t test ±SEM, n = 3 mice/condition).

(legend continued on next page)

Green fluorescent protein (GFP^+) donor cells were used to allow robust identification by FC and immunofluorescence (IF) analysis. Comparing delivery of equal numbers of NK donor cells (Figure 3A), we identified that SpNK and ThNK cells were capable of being recruited to the regenerating limb at 12 DPA, with enhanced recruitment from SpNK cells (Figures 3B–3D). 12 DPA is an important time point because the blastema has usually started to form, and histolysis is almost complete. SpNK cells show a wide distribution, whereas ThNK cells are more concentrated around the regenerating bone and dorsal nail bed (Figure 3E). Samples were co-stained for PDGFRα, a marker of MSCs (Storer and Miller, 2020), a majority cell type within the blastema with localization at the regenerating tip under the dorsal nail. SpNK and ThNK cell-treated animals show significant decreases in $PDGFR\alpha^+$ cells at 12 DPA relative to vehicle control (Figure 3E). Although fewer ThNK cells were recruited than SpNK cells (Figure 3F), the more dramatic reduction in $PDGFR\alpha^+$ cells observed with ThNK cells suggests more potent activity on blastemal progenitors.

Adoptive transfer of SpNK or ThNK cells into immunodeficient hosts reveals divergent functional activities in regeneration

Using trichrome histology and μCT imaging, distinct differences were observed with NK cell treatments of different origins. SpNK cell-treated NSG mice show accelerated regeneration, having the most complete overall morphology and largest bone volume of all treatment groups by 15 DPA (Figures 4A and 4B). In contrast, ACT of ThNK cells inhibited early wound healing, and by 12 DPA, minimal catabolism has occurred, delaying the regenerative process (Figure 4B). μCT analysis of the rate of change for each treatment showed several important differences between groups (Figure 4C). Although SpNK cell-treated groups have normal catabolism (Figures 4C and 4D), they transition to the anabolic phase quicker (Figure 4E) and have significant overgrowth of bone and an associated reduction in the final soft tissue volume at 28 DPA (Figures 4C and 4D). In contrast, ThNK cell-treated animals have impaired catabolism, never fully degrade the P3 bone (Figures 4C–4E), and have a failed anabolic phase (Figures 4D–4E). Furthermore, although soft tissue does accumulate in the blastema, this fails to differentiate into the required hard tissue (Figures 4D–4E).

ThNK cell ACT induces apoptosis coupled with a reduction in the number of osteoclasts, osteoblasts, and proliferating cells in the digit tip, whereas SpNK cell ACT induces the inverse

Treatment with SpNK cells increases osteoclast numbers, whereas ThNK cell treatment reduces osteoclast accumulation, in agreement with the inhibited catabolism *in vivo* (Figures 5A and S2). SpNK and ThNK cell treatment reduced $PDGFR\alpha^+$ cell numbers in the blastema at 12 DPA (Figure 3E); however, SpNK cell-treated animals have significantly more osteoblasts that differentiate normally from $PDGFR\alpha^+$ progenitors. Furthermore, SpNK cell-treated animals show enhanced proliferation ($PCNA^+$ and $pHH3^+$ cells) and without apoptosis (Figures 5B and 5C). OSX and pHH3 marker activation suggests that this is a region of osteogenic proliferation. In contrast, ThNK treatment results in a massive increase in $TUNEL^+$ apoptotic cells (Figures 5B and 5C) and a reduction in osteoclasts and osteoblasts. These data, together with the failure to reduce soft tissue volume (Figure 4) at the late stage of regeneration (12–28 DPA), suggest that the blastema is failing to differentiate $PDGFR\alpha^+$ progenitor cells into osteoblasts and new bone. In support of this, we observed activation of the PCNA proliferative marker in ThNK cell-treated digits but loss of mitotically active $pHH3^+$ cells, possibly suggesting that proliferating cells are becoming apoptotic before differentiating.

Ex vivo, NK cells show high cytotoxicity against RMA-S cells and Maf-DKO cell lines

We then evaluated whether ThNK and SpNK cells had intrinsic differences in cytotoxicity levels against osteoclast progenitor target cells. Cytotoxicity assays were performed by coculturing murine RMA-S or Maf-DKO cell lines with ThNK or SpNK cells with varying effector (E) NK cell to target (T) cell ratios for 4 h (1:1, 2:1, 5:1, and 10:1) (Figure 6A). The RMA-S leukemic cell line has low major histocompatibility complex (MHC) class I expression, making it a target for NK-mediated cytolytic cell death responses. SpNK cells show high cytotoxicity against control RMA-S target cells, as reported previously (Koh et al., 2001), but ThNK cells show higher endogenous killing of RMAs (Figure 6B). Osteoclasts are derived from monocyte precursor cells. Maf-DKO cells are self-renewing cells deficient in MafB/cMaf that are functionally and morphologically similar to monocytes, have the ability to differentiate

(D) μCT analysis of hard (white) and soft (teal) tissue volume over time upon NK depletion relative to saline-injected controls.
(E) Quantification of μCT volume during regeneration in the presence or absence of NK cells. Bone volume ratio (BVR) and soft tissue volume ratio (SVR) quantification were based on μCT relative to an unamputated control digit. ***$p < 0.001$, two-way ANOVA and Bonferroni ±SEM, n = 5 mice/condition).
(F) The rate of hard and soft tissue change was calculated by taking the first derivative of the change in tissue volume.

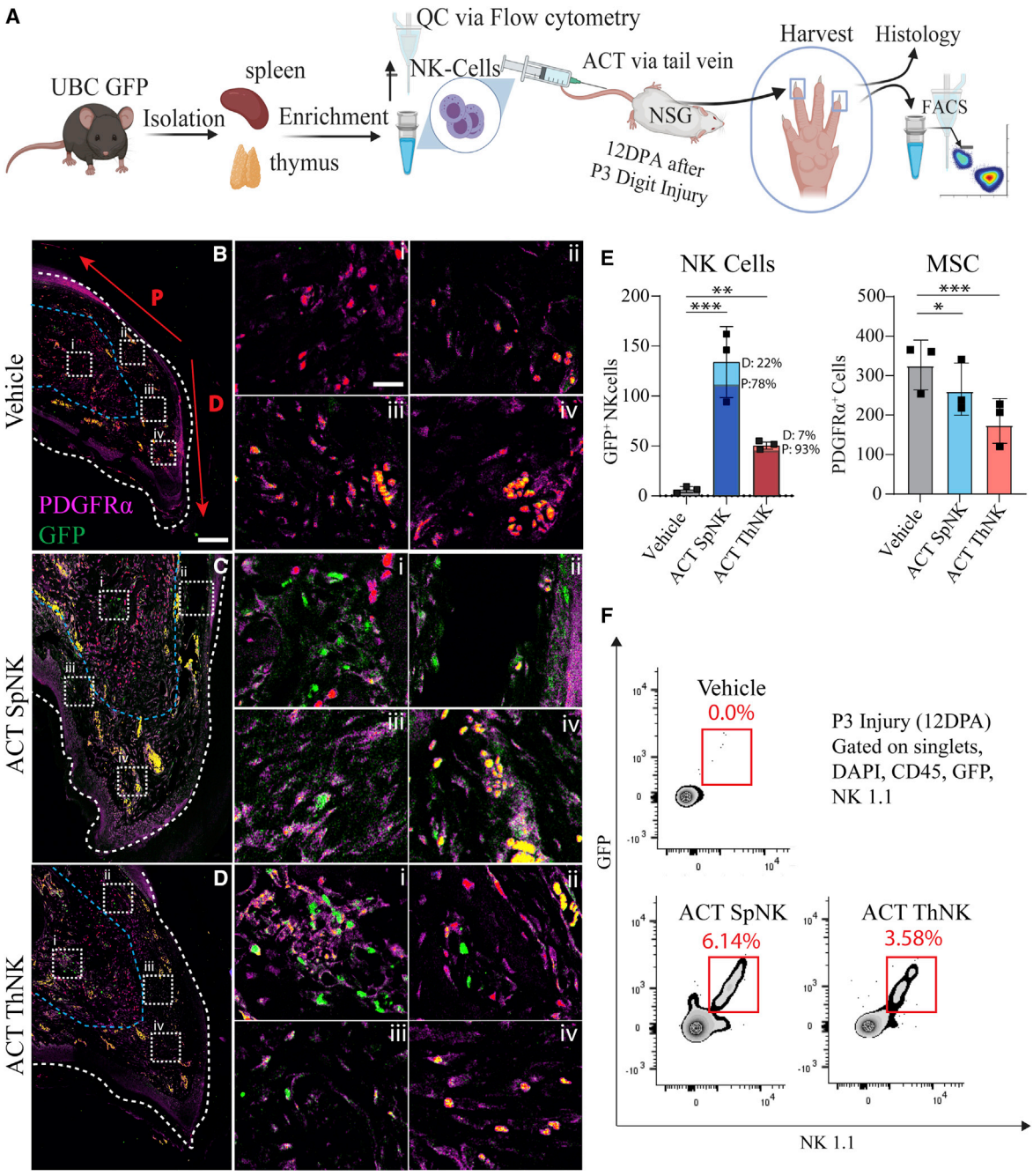

Figure 3. NK cell migration after tissue-specific ACT in an immunocompromised mouse

(A) SpNK and ThNK cells were harvested from a GFP$^+$ mice, enriched, and injected into NSG mice via adoptive cell transfer (ACT). Digit tips were collected 12 DPA after P3 amputations.

(B–D) Representative confocal microscopy with dual staining of PDGFRα$^+$ (MSCs) and NKP46$^+$ (NK cell) invasion. High-magnification insets are shown in (i)–(iv). White and blue dashed lines mark nail and soft tissue/bone boundaries, respectively. The region of distal (D) versus proximal (P) blastema used for counting is indicated in red.

(E) Digit tip NK cell or PDGFRα$^+$ (MSC) quantification via microscopy confirms migration of GFP$^+$ SpNK and ThNK cells into regenerating digit tip PDGFRα$^+$ cells relative to vehicle-injected control (*$p < 0.05$, **$p < 0.01$, ***$p < 0.001$; one-way-ANOVA and Tukey's test ±SEM; n = 3 mice/condition).

(F) FC quantification of dissociated digit tips based on antibody staining of GFP$^+$ NK1.1$^+$ NK cells (n = 20 pooled digits, 5 mice/condition).

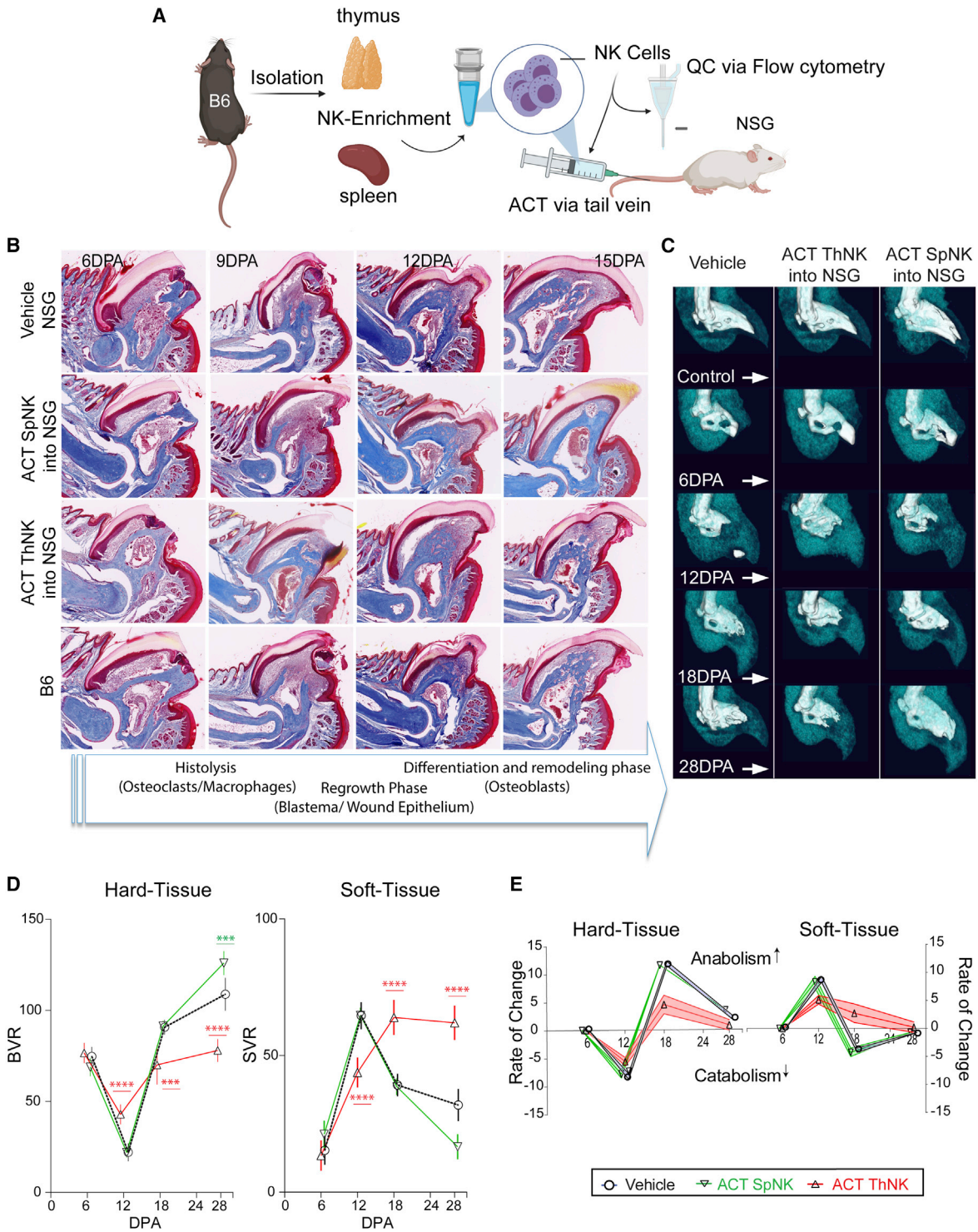

Figure 4. Adoptive transfer of SpNK or ThNK donor cells into immunodeficient hosts reveals alternative functional effects on digit tip regeneration *in vivo*

(A) SpNK and ThNK cells were harvested from C57Bl6/J (B6) mice, enriched, and injected into NSG mice via ACT.

(B) Representative trichrome histological characterization of SpNK and ThNK cell-treated NSG animals over the early time course of regeneration relative to vehicle and B6 animal controls (n = 4). Key regenerative stages are described in the arrow banner below.

(legend continued on next page)

into macrophages (Aziz et al., 2009), and are capable of forming osteoclasts *in vitro* (Nasser et al., 2020). We tested the potential for osteoclast precursor killing by NK cells via cytotoxicity assays using Maf-DKO target cells. ThNK and SpNK cells were capable of monocyte killing *in vitro,* with ThNK cells exhibiting significantly more than SpNKs (Figure 6C).

ThNK and SpNK cells are cytotoxic toward PDGFRα$^+$ progenitor cells *in vitro* and *ex vivo*

To test the potential for cytotoxicity against blastemal progenitors, ThNK cells or SpNK cells were isolated magnetically (negatively selected) from B6 mice in parallel with PDGFRα$^+$ cells isolated from the B6 mouse 12 DPA regenerating digit (Figure S3) and sorted by fluorescence-activated cell sorting (FACS) for autologous co-culture cytotoxicity assays (Figure 6D). ThNK and SpNK cells showed potent cytotoxicity against PDGFRα$^+$ blastemal target cells. To gain insights into the genetic pathways controlling NK cell cytotoxicity, we performed autologous cytotoxicity assays with 3 genetic knockout strains with altered NK cell function. The NKP46 (Ncr1) and NKG2D (Klrk1) receptors are major activation receptors licensing NK cells to kill their targets, and Prf1 is part of the lytic machinery that induces apoptosis of target cells. Cytotoxicity assays using matched donor and target animals (Ncr1$^{gfp/gfp}$, Klrk1$^{-/-}$ or Prf1$^{-/-}$ on a B6 genetic background) revealed that Ncr1-null (Ncr1$^{gfp/gfp}$) NK cells retained high cytotoxicity to levels like the parent B6 reference strain. Klrk1$^{-/-}$ and Prf1$^{-/-}$ NK cells showed significantly decreased cytotoxicity compared with Ncr1 $^{gfp/gfp}$ (Figure 6F). These findings support a model where ThNK cells could compromise blastema formation through cytotoxicity. Given that SpNK and ThNK cells had divergent functional activities *in vivo* (including differences in apoptotic cells), the finding that both are capable of cytotoxicity against osteoclast and osteoblast precursors *ex vivo* suggests that additional regulators of this process are operating *in vivo*.

ACT of NK cells from knockout models reveals tissue-origin-specific mechanisms of regeneration regulation

To gain mechanistic insights into which stages of regeneration are regulated by NK cells *in vivo*, we compared wild-type donor NK cells with mutant cells defective in NK cell signaling and effector function. Donor SpNK or ThNK cells isolated from wild-type (B6) or Klrk1$^{-/-}$, Prf1$^{-/-}$, and *Ncr1*$^{gfp/gfp}$ mutant mice produced stage-specific changes to regeneration in NSG recipient mice (Figures 7A, S1, and S3). The pro-regenerative effects of wild-type SpNK cells were not affected by loss of Prf1$^{-/-}$ (Figures 7B and 7D). Loss of Klrk1 in SpNK cells abolished any positive effect. Surprisingly, deletion of the Ncr1 gene not only eliminated the positive effect on regeneration but converted the *Ncr1*$^{-/-}$ SpNK cells into inhibitory cells in the regenerative process. The inhibitory activity of wild-type ThNK cell donors showed a more complex pattern (Figures 7C, 7E, and 7F). Final bone volume was rescued to normal (vehicle) levels in Prf1$^{-/-}$ and *Ncr1*$^{gfp/gfp}$ donors but with a delay in the anabolic bone accumulation phase and soft tissue differentiation. Klrk1$^{-/-}$ ThNK cell donors show complete rescue, with differentiation similar to or improved over vehicle control. ThNK cell inhibition of osteoclastogenesis is partially rescued in all mutant donor cells (Figure 7C). These results suggest a mechanism *in vivo* where SpNK cells enhance regeneration, mainly acting through positive regulation of new bone formation via MSC differentiation and proliferation in an Ncr1-dependent manner, where ThNK cells play an inhibitory role, acting on the catabolic and anabolic phases (Figure 7G).

DISCUSSION

Enhancing natural regeneration, activating latent endogenous regeneration, or development of successful MSC implantation therapies will rely on regulating the survival and expansion of stem progenitors and their differentiation into replacement tissues. NK cells are recruited to many wounds and have the potential to shape the healing response. Although many studies have focused on the positive roles of NK cells in producing cytokines and chemokines capable of stimulating repair, the potentially destructive role of some NK cell subsets has not been adequately addressed. In this study, we report two developmentally distinct NK cell subsets that have the potential to kill progenitor cells *ex vivo* but have divergent roles within the regenerating digit microenvironment, with ThNK cells playing a cytotoxic role affecting osteoclast and osteoblast cell progenitors. In contrast, SpNK cells showed pro-regenerative effects, resulting in enhanced osteoclast and osteoblast progenitor survival, proliferation, and differentiation. These findings suggest that NK cells are important regulators of regeneration that could be valuable future targets for enhancing repair and regeneration in human tissue.

Immunodeficient NSG mice are deficient in NK cells, T cells, and B cells but regenerate the P3 digits extremely

(C) Representative μCT images of digit tip regeneration after SpNK or ThNK cell ACT.
(D) Volumetric analysis of μCT cohorts. BVR and SVR were quantification based on μCT relative to unamputated control digits (***p < 0.001, ****p < 0.0001; two-way ANOVA and Bonferroni ±SEM; n = 5 mice/condition).
(E) Rate of change of hard and soft tissue volume, calculated by taking the first derivative of the change in tissue volume.

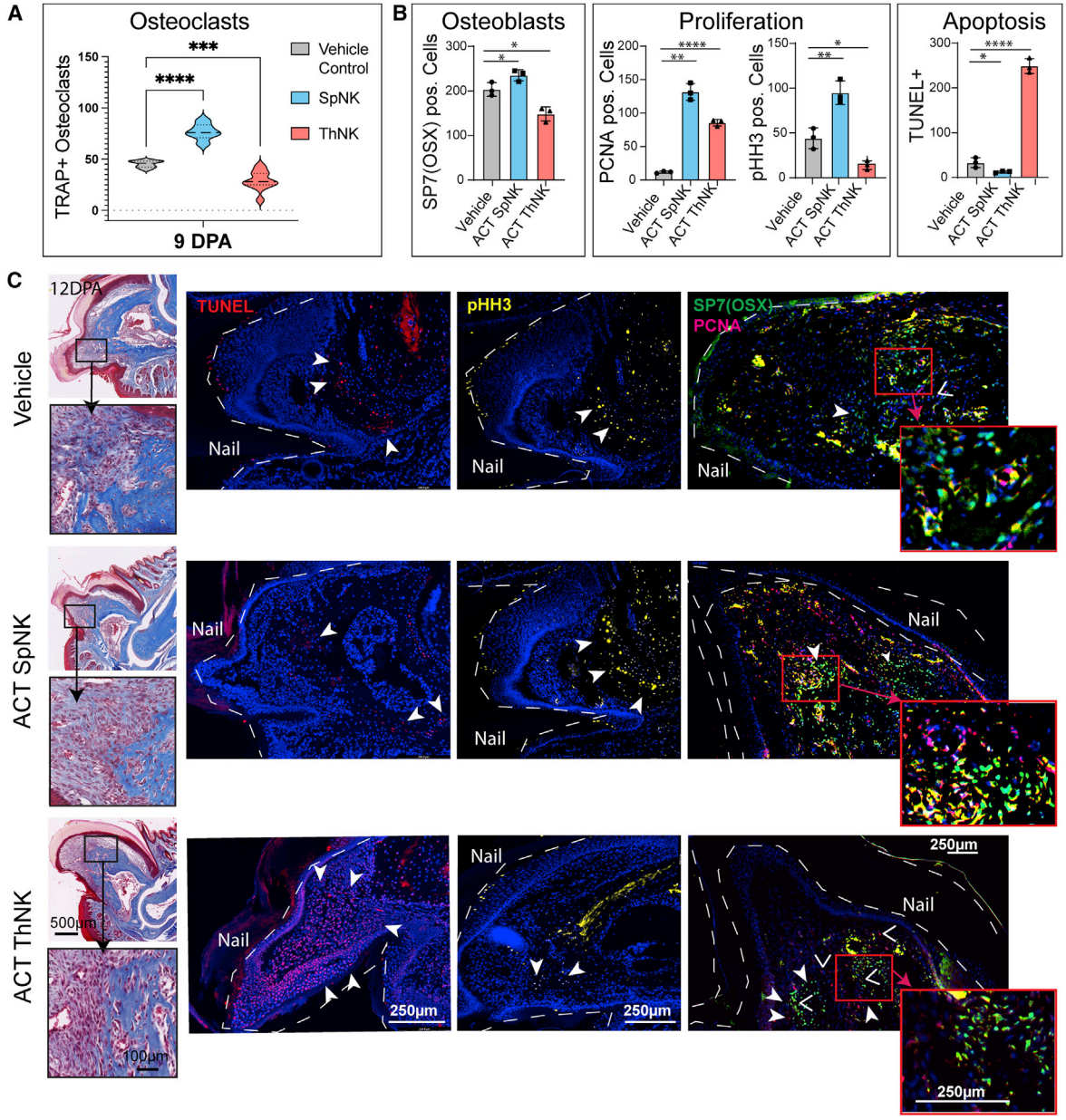

Figure 5. Adoptive transfer of SpNK or ThNK cells into NRG mice shows alternative outcomes on cell death and blastemal cell progenitors

(A) Quantification of osteoclasts (TRAP$^+$) by cytochemical staining at 9 DPA.

(B) Quantification of osteoblast cells (OSX$^+$), proliferation (PCNA$^+$, pHH3$^+$), and apoptosis (TUNEL$^+$) at 12 DPA.

(C) Trichrome staining showing the region of interest 12 DPA after P3 amputation. IF staining of TUNEL (red), pHH3 (yellow), OSX (green), and PCNA (magenta) after ACT of NK cells from the thymus and spleen and a vehicle control (n = 3). Boxes outlined in red show magnified panels at 40x. OSX$^+$ (green) and PCNA$^+$ (magenta) colocalization is indicated in yellow. *p < 0.05,**p < 0.01, ***p < 0.001, ****p < 0.0001; two-way ANOVA + Bonferroni ±SEM; n = 3 mice/condition

well, indicating that all necessary processes can occur in the absence of lymphoid cells. The inflammatory phase is associated with onset of the critical catabolic bone-degrading step at 9–12 DPA, where myeloid cells play a critical regulatory role (Simkin et al., 2017). We tested the role of NK cells in an intact immune system with transient systemic ablation of NKP46$^+$ NK cells, resulting in severe delays in regeneration and poor morphological recovery. ACT of splenic NK cells into an immunodeficient mouse (NSG) confirmed a supportive role of conventional SpNK cells in

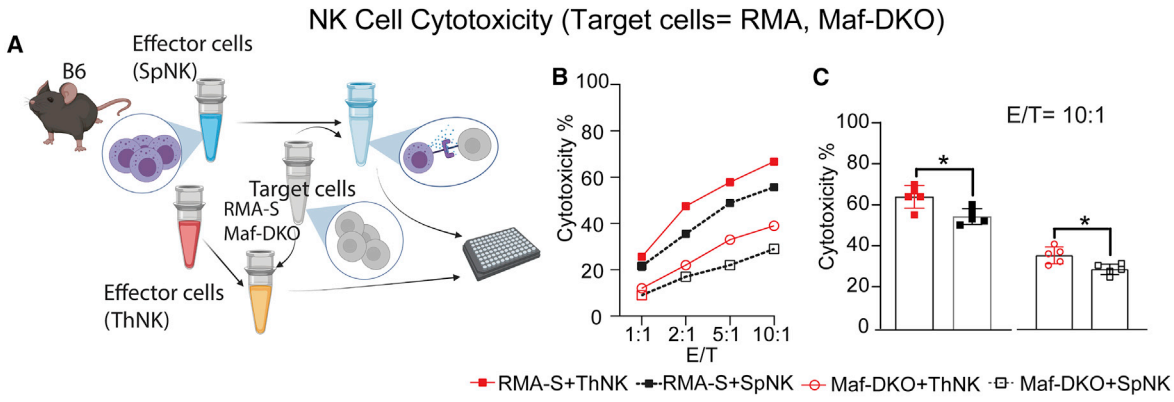

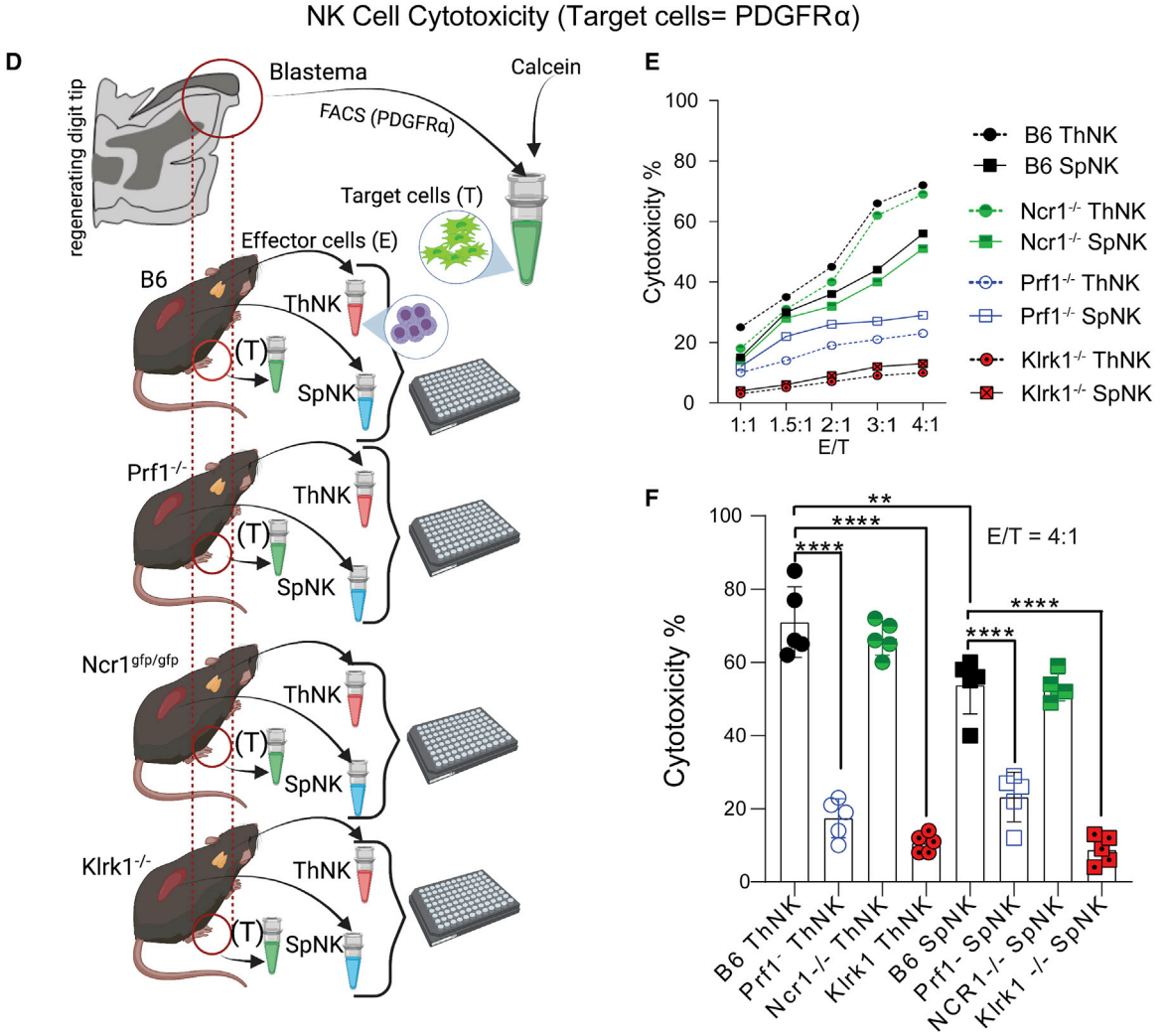

Figure 6. SpNK and ThNK donor cells show cytotoxicity against myeloid and mesenchymal cell targets *in vitro*

(A) Schematic of the effector-to-target cell cytotoxicity experiment. Effector NK cells were harvested and co-cultured with the target cell lines for 4 h (n = 3).

(B) RMA-S cells (gold-standard positive control cells sensitive to NK lysis) or Maf-DKO myeloid target cells were cultured with effector NK cells harvested from the spleen and thymus in a series of E:T ratios. RMA-S and Maf-DKO cells showed high cytotoxicity from SpNK and ThNK cells, proportional to NK cell concentration.

(legend continued on next page)

digit tip regeneration, suggesting a net positive role for NK cells in regeneration in an intact immune system.

Most reported NK cell functional studies use peripheral blood-derived NK or SpNK cells. In fracture healing, peripheral blood-derived NK cells play a role in tissue deposition through recruitment of mesenchymal progenitor cells at a later stage of fracture repair as they secrete CXCL7 (Almeida et al., 2016). In corneal epithelial abrasion injuries, SpNK cells have been found to play a positive role in healing via dendritic cells and interferon γ (IFN-γ) cytokine secretion (Gao et al., 2013). Our results are consistent with these reports. Recent work has shown that at least four distinct lineages of NK cells exist with divergent cytokine repertoires, surface receptors, gene expression, and developmental pathways (Sojka et al., 2014). Based on the limited knowledge of the functional roles of these alternative NK cell populations *in vivo,* we tested ThNK cells based on the unique GATA3-dependent alternative development pathway of ThNK cells (Sojka et al., 2014). This work identified unique inhibitory ThNK cell functions in regeneration.

NK cells can kill stem cells and cancer cells with low expression of MHC class I machinery. Although the major function for NK cells is to detect and kill abnormal, physically distressed, foreign, tumorigenic, or virally infected target cells, there is evidence that they can also damage some endogenous stem cells (Jewett et al., 2013). The NK cell decision to kill is made by interpreting activating and inhibitory ligands on the target cell with their germline–encoded receptor repertoire (Vivier et al., 2008). Following interaction with self-MHC class I, engagement of inhibitory receptors prevents autoimmune destruction of autologous cells by NK cells. CD8 T cells use the MHC class I self-antigen presentation machinery to identify cancerous or infected cells (Dhatchinamoorthy et al., 2021). CD8 T cells also kill fast-cycling epithelial, ovary, and mammary stem cells at low levels (Agudo et al., 2018). To evade CD8 T cell killing, many cancers, virally infected cells, and even slowly cycling (low-abundance) stem cells, such as hair follicle stem cells and satellite cells, can downregulate the MHC class I machinery (Agudo et al., 2018). NK cells detect MHC class 1 negative cells and kill cells that fail to express inhibitory licensing ligands (i.e., cancer cells). The receptors on NK cells controlling this requirement include major activation receptors such as NKG2D (Bauer et al., 1999) and NKP46 (Barrow et al., 2019). When the required inhibitory threshold is not met, activated NK cells can kill their targets via perforin-mediated injection of lytic granules (Backes et al., 2018) or by direct cytokine killing. MSCs and induced pluripotent stem cells (iPSCs) also express low levels of MHC class 1 (Pick et al., 2012), which makes them vulnerable to NK cell killing, with the sensitivity to attack decreasing with differentiation as MHC class 1 is upregulated (Tseng et al., 2010). Several studies have reported that MSCs could be killed by autologous or allogeneic NK cells in culture upon cytokine activation (Consentius et al., 2015; Spaggiari et al., 2006). MSCs have also been reported to suppress NK function (Petri et al., 2017; Sotiropoulou et al., 2006) *in vitro*; however, regulation of these interactions *in vivo* has yet to be defined.

The links between stem cell quiescence, antigen presentation, and immune evasion are still unclear, and studies of interactions between NK cells and stem cells *in vivo* are lacking. We reasoned that, within the process of regeneration, autologous endogenous progenitors may also be susceptible to NK cell lysis. The early phase of digit tip regeneration is regulated by the success of osteoclast progenitors. Monocytes recruited to the early wound can differentiate into osteoclasts and free-clodronate-mediated osteoclast ablation delays regeneration (Simkin et al., 2017). We found that ThNK cells inhibit osteoclast accumulation and that this delay in histolysis is partially dependent on NKP46, NKG2D, and Prf1. Other studies have reported that osteoclasts express numerous ligands for receptors present on activated NK cells (Feng et al., 2015). Co-culture experiments revealed that interleukin-15-activated but not resting blood-derived NK cells trigger osteoclast apoptosis in a dose-dependent manner (Feng et al., 2015). SpNK cells increase osteoclast numbers, but histolysis is not affected *in vivo* with deletion of NKP46, NKG2D, or Prf1, suggesting that other mechanisms regulate promotion of osteoclasts by SpNK cells. Synovial NK cells co-cultured with monocytes can trigger their differentiation into osteoclasts, and this is thought to play a role in progressive bone destruction in arthritis (Soderstrom et al., 2010). Crosstalk mechanisms between monocyte/macrophages and NK cells have

(C) Cytotoxicity at an E:T/ratio of 10:1. RMA-S and Maf-DKO cells show significantly higher cytotoxicity in the presence of ThNK cells compared with SpNK cells.

(D) Schematic of autologous PDGFRα$^+$ cell versus NK cell (ThNK or SpNK cell) isolation and cytotoxicity assays in mutant and control mice. Fluorescence-activated cell sorting (FACS) of mesenchymal PDGFRα$^+$ cells from Prf1 KO, Ncr1^{gfp}, Klrk1$^-$, and B6 after P3 injury (9 DPA) was performed. SpNK or ThNK effector cells were isolated and matched with the original PDGFRα$^+$ target (autologous) cell source.

(E) NK cell cytotoxicity toward PDGFRα$^+$ cells after co-culture.

(F) Prf1 and *Klrk1* KO donors (SpNK and ThNK cells) have significantly reduced cytotoxicity against PDGFRα$^+$ target cells at an E:T ratio of 4:1. *Ncr1* KO cytotoxicity remains similar to B following treatment with NK cells. Statistics were performed using Student's t test (*p < 0.05) for two groups and one-way ANOVA and Tukey's test ±SEM for three or more groups; n = 5. **p < 0.01, ****p < 0.0001).

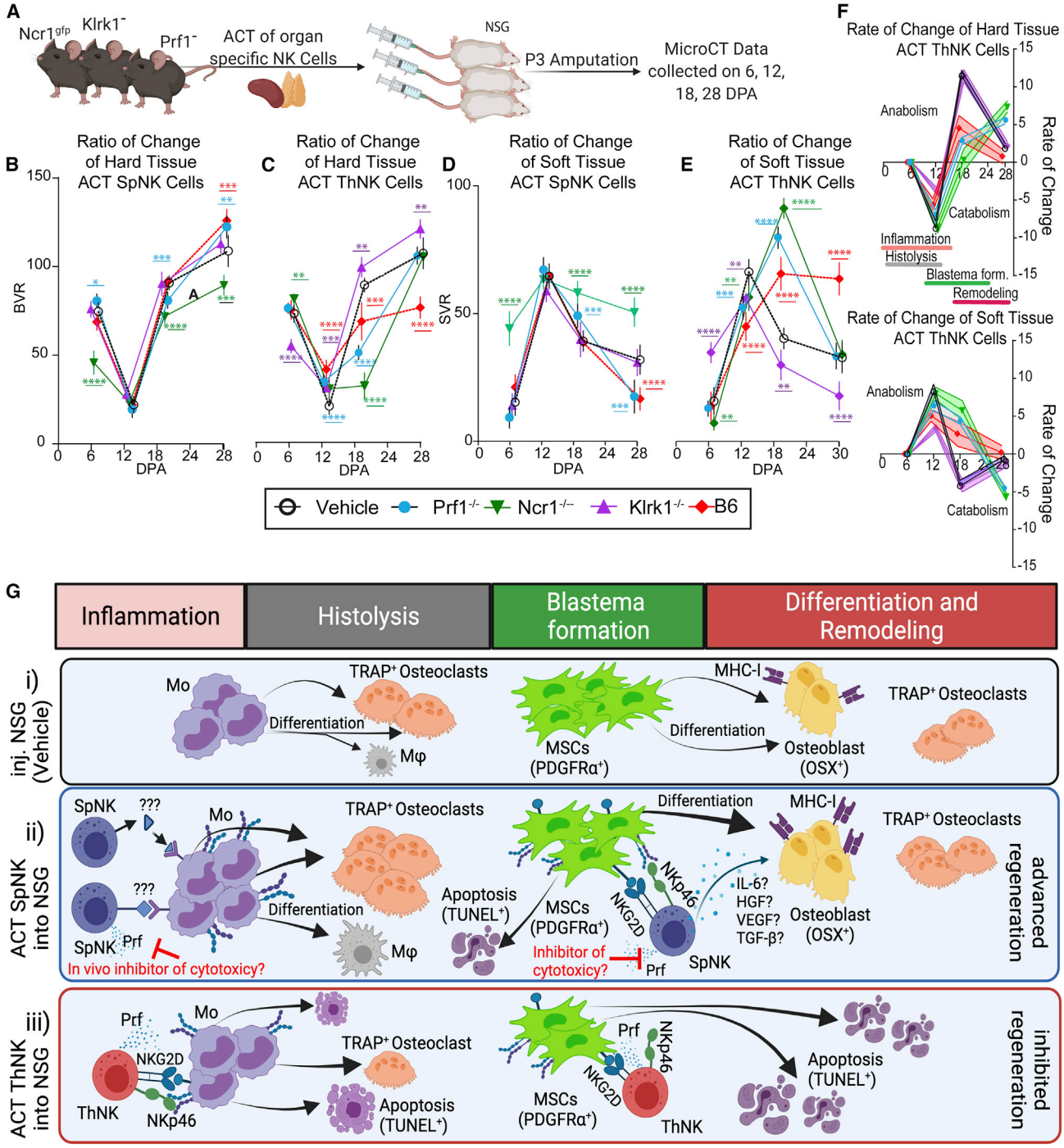

Figure 7. Adoptive transfer of NKP46-, NKG2D-, and perforin-deficient donor NK cells identifies NK cell subset-specific mechanisms of regenerative regulation

(A) The effect of donor NK cells from NKP46 (*Ncr1*$^{gfp/gfp}$), NKG2D (*Klrk1*$^{-/-}$), perforin (Prf1$^{-/-}$), and B_6 mice on NSG P3 digit regeneration.

(B–E) Volumetric μCT analysis of each NK donor cell cohort relative to unamputated control digits. A red line shows the effect of wild-type SpNK or ThNK cell adoptive transfer. A black line shows normal regeneration without any NK cells (vehicle). Mutant donor cells are indicated by the legend color code. *p < 0.05, **p < 0.01, ***p < 0.001, ****p < 0.0001; two-way ANOVA Bonferroni ±SEM; n = 5 mice.

(C and D) BVR.

(E and F) SVR.

(legend continued on next page)

been identified, but interactions regulating osteoclastogenesis in repair are still emerging (Michel et al., 2013).

Our study tested the effect of ThNK and SpNK cells on recruitment, survival proliferation, and differentiation of PDGFRα$^+$ progenitor cells into osteoblasts. ThNK cell induction of apoptosis provides strong evidence of NK-mediated destruction of proliferating endogenous stem cell progenitor cells *in vivo*. The presence of NK cells near the nail epithelium could also suggest NK cell regulation of progenitor cell migration into the blastema. PDGFRα$^+$ cells are known to reduce MHC class I to function as an MSC, whereas the NKG2D receptor is known to induce apoptosis in cells with decreased MHC class I (Trapani and Smyth, 2002). In the absence of NKG2D, ThNK cell inhibition is eliminated, suggesting that PDGFRα$^+$ cells may be eliminated by NKG2D-dependent NK killing and not survive to differentiate into new bone. The potent reduction of mitotic (pHH3$^+$) cells in ThNK cell-treated digits was not accompanied by a reduction in PCNA$^+$ cells. Although PCNA is a common proliferation marker, this protein is also an inhibitory ligand for NKP44 activation (Rosental et al., 2011). It is possible that this mechanism of inhibition may not be available to ThNK cells because we found a potent reduction in mitotically active cells within blastemas treated with ThNK cells. Evidence in the literature suggests that mitotic cells undergo heightened NK cell surveillance and are more susceptible to NK cell cytotoxicity (Nolte-'t Hoen et al., 2007), with important implications for regeneration. Previous observations in liver regeneration models support our findings. NK cell ablation prior to partial hepatectomy results in liver overgrowth, suggesting a role of NK cells in regulating this regenerative process (Vujanovic et al., 1995). Transient increases in liver hepatocyte susceptibility to lysis by liver-resident NK cells is limited to the period of rapid liver growth, and early liver regeneration is facilitated by suppression of cytotoxicity in local but not remote NK cell sources.

Although SpNK cells show high Prf1- and Klrk1-dependent cytotoxicity against *ex vivo* PDGFRα$^+$ progenitor cells in culture, the lack of apoptosis or osteoblast inhibition *in vivo* indicates that they undergo additional regulation. Fracture exudate is suppressive of cytotoxicity of blood-derived NK cells, which may facilitate repair (Hauser et al., 1997), and the blastema wound may impose similar regulation. Wound suppression of NK cell cytotoxicity is ineffective against ThNK cells because they induce massive apoptosis and reduces the number of PDGFRα$^+$ progenitors, osteoblasts, and mitotically active cells. This suggests that cytotoxicity is regulated differently in NK cell subsets from different tissue and developmental origins. Although SpNK cells decrease PDGFRα$^+$ cell numbers, at 12 DPA this is associated with enhanced mitotically active (pHH3$^+$) cell and osteoblast numbers with reduced rates of apoptosis. We interpret these findings as SpNK cell enhancement of PDGFRα$^+$ cell proliferation and differentiation into osteoblasts with low cytotoxicity. The SpNK cell pro-regenerative properties are abolished with Klrk1 deletion where Prf1 deletion had no effect *in vivo*. The observation that pro-regenerative SpNK cells can be converted to inhibitory cells when they lack the NKP46 receptor suggests that this receptor is a major regulator of NK cell function. In support of this finding, the NKP46 receptor (Ncr1) is known to regulate NK cell lysis of autologous, allogeneic, or xenogeneic cells via MHC class 1-independent mechanisms (Sivori et al., 1999).

This report has identified NK cells as key regulators of digit tip regeneration process, where the tissue source of the NK cells determines function within the blastema. ThNK and SpNK cells show opposing roles in regulation of osteoclastogenesis and survival, proliferation, and differentiation of mesenchymal progenitor cells. To what extent inhibitory ThNK cells may be counterbalanced by pro-regenerative SpNKs in various injury contexts may determine limits in regeneration potential. The lack of *in vivo* studies using NK cells from divergent tissue origins has been a limiting factor in fully appreciating the range of functional activities of NK cells but demonstrate the importance of NK lineage and tissue origin in regulating regeneration. The findings that endogenous stem cell survival, proliferation, and differentiation are regulated in divergent ways by developmentally distinct NK cell subsets are likely to be significant in various contexts. Further studies are required to elucidate the mechanisms that regulate progenitor cell protection in wound repair regeneration. A full understanding of NK cell-progenitor cell interactions may

(F) First derivative of the ratio of change of hard and soft tissue volume after ThNK cell ACT. Phases of regeneration are shown. All statistical analyses are shown relative to vehicle (n = 5).

(G) Model of NK cell subset effects at different stages of regeneration *in vivo*. (i) NSG mice lacking NK cells undergo normal monocyte (Mo) differentiation into osteoclasts and normal osteoblast differentiation from MSC progenitors. Late-phase osteoclast-osteoblast interactions promote remodeling and comprehensive regeneration. (ii) ACT of SpNK cells enhances osteoclast differentiation and early transition to anabolism by promoting MSCs proliferation and differentiation into osteoblasts via cytokines and NKP46 and NKG2D receptor interactions. SpNK cell cytotoxicity is suppressed *in vivo* with minimal apoptotic activation. (iii) ACT of ThNK cells inhibits regeneration via cytotoxicity. ThNK cells inhibit osteoclast differentiation or survival, partially dependent on NKP46, NKG2D, and Prf1. ThNK cells inhibit proliferation, differentiation, and survival of MSCs and osteoblasts, leading to failed outgrowth and catastrophic apoptosis.

lead to clinical improvements in treatment of disease or new approaches for regenerative medicine.

EXPERIMENTAL PROCEDURES

Animals and digit tip amputations

All animal experiments were carried out according to procedures approved by The Jackson Laboratory Animal Care and Use Committee (ACUC). The following mouse stocks were obtained from The Jackson Laboratory: (B6)C57BL/6J-#000664, (NSG) #005557, ($Ncr1^{gfp}$), #022739, (Prf1 knockout [KO])#022739, ($Klrk1^{-}$) # 022733, and (UBC-GFP) # 004353. $Ncr1^{tm1.1(icre)Viv}$ (MGI:5308410) mice were a kind gift from Eric Vivier and Stephen Waggoner. NKP46 DTR mice were generated by intercrossing $Ncr1^{tm1.1(icre)Viv}$ (MGI:5308410) with $ROSA^{DTR}$ (MGI:3772576) mice. P3 amputations performed on age-matched 8- to 10-week-old male mice anesthetized with isoflurane before amputation of the distal third of the terminal phalanges (Storer and Miller, 2020). Two digits per hindpaw were amputated, with the middle digit used as an uninjured control (Figure 1A). Buprenorphine was given at 1 mg/kg via a subcutaneous injection. After amputation, the digits were sprayed with Cavilon No-Sting Barrier Film (3M) to minimize potential infection. For $NKP46^{+}$ cell depletion in NKP46 DTR mice, 200 ng DT was injected intravenously (i.v.) at 3-day intervals. Blastemal cells were isolated via mechanical dissociation on glass dishes (MatTek, P35G-0-10-C) and then digested with 1 U/mL Liberase-DH (Roche, 5401054001) in tubes for 60 min at 37°C. Dissociated cells were used for FC and cytotoxicity assays.

μCT scans and image processing

μCT imaging was performed using a Quantum GX μCT (PerkinElmer) at high resolution (voxel size, 10 μm; energy, 55 kVp; 1,000 projections per 180° captured in 380 ms using continuous rotation) using methods described previously (Simkin et al., 2017). Briefly, μCT files were reconstructed using ImageJ and the BoneJ (version 1.2.1) Optimized Threshold plugin to produce 3D renderings. We used contrast settings for hard tissue (85%) and soft tissue (15%). Images were cropped to the base of the nail bed for soft tissue and whole P3 bone for hard tissue. Volume measurements were made using the MorphoLibJ plugin under default settings.

Magnetic purification of leukocytes and FC

The MojoSort Mouse NK Cell Isolation Enrichment Kit (BioLegend, 480050) was used to isolate untouched NK cells. Adoptive NK cell transfer into NSG hosts was performed via tail vein injection with a 1:1 donor:recipient ratio. Magnetic enrichment was validated by FC prior to ACT for each purification. Typical purifications were 85–95% pure. Flow cytometry (FC) was performed by treating cells with an Fc-Shield antibody cocktail (αCD16/αCD32) in FACS buffer (Hank's balanced salt solution [HBSS], 5 mM EDTA, and 2% fetal calf serum [FCS]) using the following antibodies (1:400 dilution): anti-mouse $CD45^{-}$ PE-Cy7 (BD Biosciences, 559864), NK 1.1-BV 785 (BD Biosciences, 108749), and NKP46- BV 421 (BD Biosciences, 562850) for 60 min on ice. Cells were washed and centrifuged at 400 × *g* for 7 min twice. Cells were stained with 4′,6-diamidino-2-phenylindole (DAPI) and analyzed on a FACSymphony A5 cytometer (BD Biosciences, San Jose, CA, USA). Data were analyzed with FlowJo version 10 (Tree Star, Ashland, OR, USA).

IF

IF staining was performed as described previously (Simkin et al., 2017). Briefly, mice were perfused in PBS. Digit tips were fixed in zinc-buffered formalin (Z-fix, Anatech, NC9378601) for 24 h. Decalcification was performed in Surgipath decalcifier I (Leica, 3800400) for 24 h at 4°C, then washing in PBS and transferring to 70% ethanol before embedding in paraffin. 5 μM sections were air dried overnight prior to antigen retrieval using citrate buffer (pH 6) in an IHC-Tek Epitope Retrieval Steamer for 20 min. Sections were blocked using 5% BSA in PBS containing 0.3% Triton X-100 for 1 h at room temperature and then stained. For paraffin IF staining, samples were treated with Trueblack (Biotium, 23007) according to the manufacturer's instructions and stained 1:200 with the following antibodies: phospho-histone H3 (Invitrogen, 44-1190G), PCNA (Dako, M0879), and NKP46 (Invitrogen, PA5102860). Detection was performed using goat anti-rabbit 647 (Invitrogen, A21244) and/or goat anti-mouse 568 (Invitrogen, A11031). TUNEL staining was performed using the Click-iT TUNEL Alexa Fluor 647 Imaging Assay (C10247). Sections were counterstained with DAPI for 10 min. All 2D images were collected with a point scanning confocal microscope (LSM 980, Carl Zeiss, Germany, or SP8-X, Leica, Switzerland) with Zen Blue software or Leica LAS X LS. All imaging parameters were identical between samples.

Masson trichrome and TRAP staining

To measure $TRAP^{+}$ osteoclasts, paraffin sections were deparaffinized and incubated in acetate-tartaric acid buffer (0.2 M sodium acetate [Merck, 6268], 50 mM tartaric acid [Sigma-Aldrich, T10-9], pH 5.0) for 20 min at 37°C and then stained in 1.1 mg/mL FAST Red TR (Sigma, F8764-16) substrate and 0.1–0.5 mg/mL napthol ASMX phosphate (Sigma, N4875) substrate. Sections were incubated for 2–4 h until sufficient red color was observed in osteoclasts, washed in PBS, and then counterstained with Methyl Green (Vector Laboratories, H-3402-500) before washing, air drying, and mounting in VectaMount permanent mounting medium (Vector Laboratories, H-50000). Masson trichrome staining was performed using the Masson Trichrome Stain Kit (SKU KTMTRLT EA, StatLab, TX, USA) according to the manufacturer's instructions. Images were obtained using a Zeiss Colibri inverted microscope at 10x and 20x dry magnification using a Zeiss 305 color camera.

Assay measuring NK cell cytotoxicity

The murine T cell lymphoma cell line RMA-S (H-2b; ATCC, Rockville, MD), Maf-DKO cells (Aziz et al., 2009), and target cells (RMAs, DKO, and primary sorted PDFGRα cells from B6 mice) were seeded at varying densities (1×10^3 to 1×10^5 cells/mL) in DMEM with in black-walled 96-well plates. Target cells were stained with 5 μM Calcein blue AM (Thermo Fisher Scientific, C34853) and 2.5 μM propidium iodide (PI) for 30 min, washed 3 times with DMEM, and loaded with Fluoborite (Thermo Fisher Scientific, A1896701). Effector cells (SpNK and ThNK cells) were isolated from 8-week-old B6 mice and co-cultured at different concentrations with the target cells. Fluorescence was measured using a

SpectraMax iD3 Multi-Mode Microplate Reader. Calcein blue AM was recorded using a 323/439-nm filter. PI was recorded using a 535/617-nm filter. Output was quantified via a standard curve. Cytotoxicity was calculated by dividing the ratio of Calcein blue to PI of treated cells by the ratio of the control cells and subtracting from 1.

Statistical analysis

Statistical analysis was performed using GraphPad Prism 9 (GraphPad, La Jolla, CA, USA; version 8.4.3) as indicated. Coding of samples and blinding were done when possible.

SUPPLEMENTAL INFORMATION

Supplemental information can be found online at https://doi.org/10.1016/j.stemcr.2022.01.006.

AUTHOR CONTRIBUTIONS

N.D. performed digit tip surgeries, microscopy, μCT analysis, NK and MSC cell purification, adoptive transfer of purified cells, and data interpretation and edited the manuscript. Z.B. performed μCT imaging and analysis and adoptive transfer of purified cells, assisted with experimental design, analyzed data, and edited the manuscript. J.G. conceived the study, generated the hypothesis, designed the experiments, analyzed data, and wrote and edited the manuscript.

CONFLICT OF INTERESTS

The authors declare no competing interests.

ACKNOWLEDGMENTS

We acknowledge the JAX Center for Biometric Analysis for instrumentation, training, and technical support with μCT imaging (Doug Morris and Christine Wooley), the JAX imaging core and MDIBL Light Microscopy Facility (Frédéric Bonnet), and the JAX Flow Cytometry Core for support (Will Schott); we also acknowledge JAX Histology Services (Elaine Bechtel) for technical support. We wish to thank Michael Sieweke, Eric Vivier, Stephen Waggoner, and Derry Roopenian for critical mouse cell lines and animals and Nadia Rosenthal for critical infrastructure support. We thank Lilian Hyde for flow cytometry assistance and Khaled Dastagir for advice regarding cytotoxicity assays and μCT volumetric analysis. We thank Dustin Updike and Andrew Walter for careful reading of the manuscript. We gratefully acknowledge funding from the German Research Foundation (DFG), JAX institutional support, and funds from the National Institute of General Medical Sciences of the National Institutes of Health (NIGMS) under grants P20GM0103423 and P20GM104318 (to J.G. and MDIBL).

Received: November 23, 2021
Revised: January 6, 2022
Accepted: January 7, 2022
Published: February 3, 2022

REFERENCES

Agudo, J., Park, E.S., Rose, S.A., Alibo, E., Sweeney, R., Dhainaut, M., Kobayashi, K.S., Sachidanandam, R., Baccarini, A., Merad, M., and Brown, B.D. (2018). Quiescent tissue stem cells evade immune surveillance. Immunity *48*, 271–285.e275. https://doi.org/10.1016/j.immuni.2018.02.001.

Almeida, C.R., Caires, H.R., Vasconcelos, D.P., and Barbosa, M.A. (2016). NAP-2 secreted by human NK cells can stimulate mesenchymal stem/stromal cell recruitment. Stem Cell Reports *6*, 466–473. https://doi.org/10.1016/j.stemcr.2016.02.012.

Aziz, A., Soucie, E., Sarrazin, S., and Sieweke, M.H. (2009). MafB/c-Maf deficiency enables self-renewal of differentiated functional macrophages. Science *326*, 867–871. https://doi.org/10.1126/science.1176056.

Backes, C.S., Friedmann, K.S., Mang, S., Knorck, A., Hoth, M., and Kummerow, C. (2018). Natural killer cells induce distinct modes of cancer cell death: discrimination, quantification, and modulation of apoptosis, necrosis, and mixed forms. J. Biol. Chem. *293*, 16348–16363. https://doi.org/10.1074/jbc.RA118.004549.

Barrow, A.D., Martin, C.J., and Colonna, M. (2019). The natural cytotoxicity receptors in Health and disease. Front. Immunol. *10*, 909. https://doi.org/10.3389/fimmu.2019.00909.

Bauer, S., Groh, V., Wu, J., Steinle, A., Phillips, J.H., Lanier, L.L., and Spies, T. (1999). Activation of NK cells and T cells by NKG2D, a receptor for stress-inducible MICA. Science *285*, 727–729. https://doi.org/10.1126/science.285.5428.727.

Consentius, C., Reinke, P., and Volk, H.D. (2015). Immunogenicity of allogeneic mesenchymal stromal cells: what has been seen in vitro and in vivo? Regen. Med. *10*, 305–315. https://doi.org/10.2217/rme.15.14.

Dawson, L.A., Simkin, J., Sauque, M., Pela, M., Palkowski, T., and Muneoka, K. (2016). Analogous cellular contribution and healing mechanisms following digit amputation and phalangeal fracture in mice. Regeneration *3*, 39–51. https://doi.org/10.1002/reg2.51.

Dhatchinamoorthy, K., Colbert, J.D., and Rock, K.L. (2021). Cancer immune evasion through loss of MHC Class I antigen presentation. Front. Immunol. *12*, 636568. https://doi.org/10.3389/fimmu.2021.636568.

Fauriat, C., Long, E.O., Ljunggren, H.G., and Bryceson, Y.T. (2010). Regulation of human NK-cell cytokine and chemokine production by target cell recognition. Blood *115*, 2167–2176. https://doi.org/10.1182/blood-2009-08-238469.

Feng, S., Madsen, S.H., Viller, N.N., Neutzsky-Wulff, A.V., Geisler, C., Karlsson, L., and Soderstrom, K. (2015). Interleukin-15-activated natural killer cells kill autologous osteoclasts via LFA-1, DNAM-1 and TRAIL, and inhibit osteoclast-mediated bone erosion in vitro. Immunology *145*, 367–379. https://doi.org/10.1111/imm.12449.

Gao, Y., Li, Z., Hassan, N., Mehta, P., Burns, A.R., Tang, X., and Smith, C.W. (2013). NK cells are necessary for recovery of corneal CD11c+ dendritic cells after epithelial abrasion injury. J. Leukoc. Biol. *94*, 343–351. https://doi.org/10.1189/jlb.1212633.

Godwin, J.W., Pinto, A.R., and Rosenthal, N.A. (2013). Macrophages are required for adult salamander limb regeneration. Proc. Natl. Acad. Sci. U S A *110*, 9415–9420.

Haspeslagh, E., van Helden, M.J., Deswarte, K., De Prijck, S., van Moorleghem, J., Boon, L., Hammad, H., Vivier, E., and Lambrecht, B.N. (2018). Role of NKP46(+) natural killer cells in house dust mite-driven asthma. EMBO Mol. Med. *10*, e8657. https://doi.org/10.15252/emmm.201708657.

Hauser, C.J., Joshi, P., Jones, Q., Zhou, X., Livingston, D.H., and Lavery, R.F. (1997). Suppression of natural killer cell activity in patients with fracture/soft tissue injury. Arch. Surg. *132*, 1326–1330. https://doi.org/10.1001/archsurg.1997.01430360072013.

Jewett, A., Man, Y.G., and Tseng, H.C. (2013). Dual functions of natural killer cells in selection and differentiation of stem cells; role in regulation of inflammation and regeneration of tissues. J. Cancer *4*, 12–24. https://doi.org/10.7150/jca.5519.

Koh, C.Y., Blazar, B.R., George, T., Welniak, L.A., Capitini, C.M., Raziuddin, A., Murphy, W.J., and Bennett, M. (2001). Augmentation of antitumor effects by NK cell inhibitory receptor blockade in vitro and in vivo. Blood. J. Am. Soc. Hematol. *97*, 3132–3137.

Lehoczky, J.A., and Tabin, C.J. (2015). Lgr6 marks nail stem cells and is required for digit tip regeneration. Proc. Natl. Acad. Sci. U S A *112*, 13249–13254. https://doi.org/10.1073/pnas.1518874112.

Liippo, J., Toriseva, M., and Kähäri, V.-M. (2010). Chapter Thirty-Nine - natural killer cells in wound healing. In Natural Killer Cells, M.T. Lotze and A.W. Thomson, eds. (Academic Press), pp. 519–525. https://doi.org/10.1016/B978-0-12-370454-2.00039-9.

Michel, T., Hentges, F., and Zimmer, J. (2013). Consequences of the crosstalk between monocytes/macrophages and natural killer cells. Front. Immunol. *3*, 403.

Nasser, H., Adhikary, P., Abdel-Daim, A., Noyori, O., Panaampon, J., Kariya, R., Okada, S., Ma, W., Baba, M., Takizawa, H., et al. (2020). Establishment of bone marrow-derived M-CSF receptor-dependent self-renewing macrophages. Cell Death Discov. *6*, 63. https://doi.org/10.1038/s41420-020-00300-3.

Nolte-'t Hoen, E.N., Almeida, C.R., Cohen, N.R., Nedvetzki, S., Yarwood, H., and Davis, D.M. (2007). Increased surveillance of cells in mitosis by human NK cells suggests a novel strategy for limiting tumor growth and viral replication. Blood *109*, 670–673. https://doi.org/10.1182/blood-2006-07-036509.

Petri, R.M., Hackel, A., Hahnel, K., Dumitru, C.A., Bruderek, K., Flohe, S.B., Paschen, A., Lang, S., and Brandau, S. (2017). Activated tissue-resident mesenchymal stromal cells regulate natural killer cell immune and tissue-regenerative function. Stem Cell Reports *9*, 985–998. https://doi.org/10.1016/j.stemcr.2017.06.020.

Pick, M., Ronen, D., Yanuka, O., and Benvenisty, N. (2012). Reprogramming of the MHC-I and its regulation by NFkappaB in human-induced pluripotent stem cells. Stem Cells *30*, 2700–2708. https://doi.org/10.1002/stem.1242.

Rinkevich, Y., Lindau, P., Ueno, H., Longaker, M.T., and Weissman, I.L. (2011). Germ-layer and lineage-restricted stem/progenitors regenerate the mouse digit tip. Nature *476*, 409–413. https://doi.org/10.1038/nature10346.

Rosental, B., Brusilovsky, M., Hadad, U., Oz, D., Appel, M.Y., Afergan, F., Yossef, R., Rosenberg, L.A., Aharoni, A., Cerwenka, A., et al. (2011). Proliferating cell nuclear antigen is a novel inhibitory ligand for the natural cytotoxicity receptor NKP44. J. Immunol. *187*, 5693–5702. https://doi.org/10.4049/jimmunol.1102267.

Seifert, A.W., and Muneoka, K. (2018). The blastema and epimorphic regeneration in mammals. Dev. Biol. *433*, 190–199. https://doi.org/10.1016/j.ydbio.2017.08.007.

Simkin, J., Sammarco, M.C., Marrero, L., Dawson, L.A., Yan, M., Tucker, C., Cammack, A., and Muneoka, K. (2017). Macrophages are required to coordinate mouse digit tip regeneration. Development *144*, 3907–3916.

Sivori, S., Pende, D., Bottino, C., Marcenaro, E., Pessino, A., Biassoni, R., Moretta, L., and Moretta, A. (1999). NKP46 is the major triggering receptor involved in the natural cytotoxicity of fresh or cultured human NK cells. Correlation between surface density of NKP46 and natural cytotoxicity against autologous, allogeneic or xenogeneic target cells. Eur. J. Immunol. *29*, 1656–1666. https://doi.org/10.1002/(SICI)1521-4141(199905)29:05<1656::AID-IMMU1656>3.0.CO;2-1.

Soderstrom, K., Stein, E., Colmenero, P., Purath, U., Muller-Ladner, U., de Matos, C.T., Tarner, I.H., Robinson, W.H., and Engleman, E.G. (2010). Natural killer cells trigger osteoclastogenesis and bone destruction in arthritis. Proc. Natl. Acad. Sci. U S A *107*, 13028–13033. https://doi.org/10.1073/pnas.1000546107.

Sojka, D.K., Plougastel-Douglas, B., Yang, L., Pak-Wittel, M.A., Artyomov, M.N., Ivanova, Y., Zhong, C., Chase, J.M., Rothman, P.B., Yu, J., et al. (2014). Tissue-resident natural killer (NK) cells are cell lineages distinct from thymic and conventional splenic NK cells. eLife *3*, e01659. https://doi.org/10.7554/eLife.01659.

Sotiropoulou, P.A., Perez, S.A., Gritzapis, A.D., Baxevanis, C.N., and Papamichail, M. (2006). Interactions between human mesenchymal stem cells and natural killer cells. Stem Cells *24*, 74–85. https://doi.org/10.1634/stemcells.2004-0359.

Spaggiari, G.M., Capobianco, A., Becchetti, S., Mingari, M.C., and Moretta, L. (2006). Mesenchymal stem cell-natural killer cell interactions: evidence that activated NK cells are capable of killing MSCs, whereas MSCs can inhibit IL-2-induced NK-cell proliferation. Blood *107*, 1484–1490. https://doi.org/10.1182/blood-2005-07-2775.

Storer, M.A., and Miller, F.D. (2020). Cellular and molecular mechanisms that regulate mammalian digit tip regeneration. Open Biol. *10*, 200194. https://doi.org/10.1098/rsob.200194.

Storer, M.A., Mahmud, N., Karamboulas, K., Borrett, M.J., Yuzwa, S.A., Gont, A., Androschuk, A., Sefton, M.V., Kaplan, D.R., and Miller, F.D. (2020). Acquisition of a unique mesenchymal precursor-like blastema state underlies successful adult mammalian digit tip regeneration. Dev. Cell *52*, 509–524.e9. https://doi.org/10.1016/j.devcel.2019.12.004.

Tosello-Trampont, A., Surette, F.A., Ewald, S.E., and Hahn, Y.S. (2017). Immunoregulatory role of NK cells in tissue inflammation and regeneration. Front. Immunol. *8*, 301.

Trapani, J.A., and Smyth, M.J. (2002). Functional significance of the perforin/granzyme cell death pathway. Nat. Rev. Immunol. *2*, 735–747.

Tseng, H.C., Arasteh, A., Paranjpe, A., Teruel, A., Yang, W., Behel, A., Alva, J.A., Walter, G., Head, C., Ishikawa, T.O., et al. (2010). Increased lysis of stem cells but not their differentiated cells by natural killer cells; de-differentiation or reprogramming activates NK cells. PLoS One *5*, e11590. https://doi.org/10.1371/journal.pone.0011590.

Vivier, E., Tomasello, E., Baratin, M., Walzer, T., and Ugolini, S. (2008). Functions of natural killer cells. Nat. Immunol. *9*, 503–510.

Vujanovic, N.L., Polimeno, L., Azzarone, A., Francavilla, A., Chambers, W.H., Starzl, T.E., Herberman, R.B., and Whiteside, T.L. (1995). Changes of liver-resident NK cells during liver regeneration in rats. J. Immunol. *154*, 6324–6338.

Stem Cell Reports, Volume *17*

Supplemental Information

Tissue origin of cytotoxic natural killer cells dictates their differential roles in mouse digit tip regeneration and progenitor cell survival

Nadjib Dastagir, Zachery Beal, and James Godwin

Supplementary Information

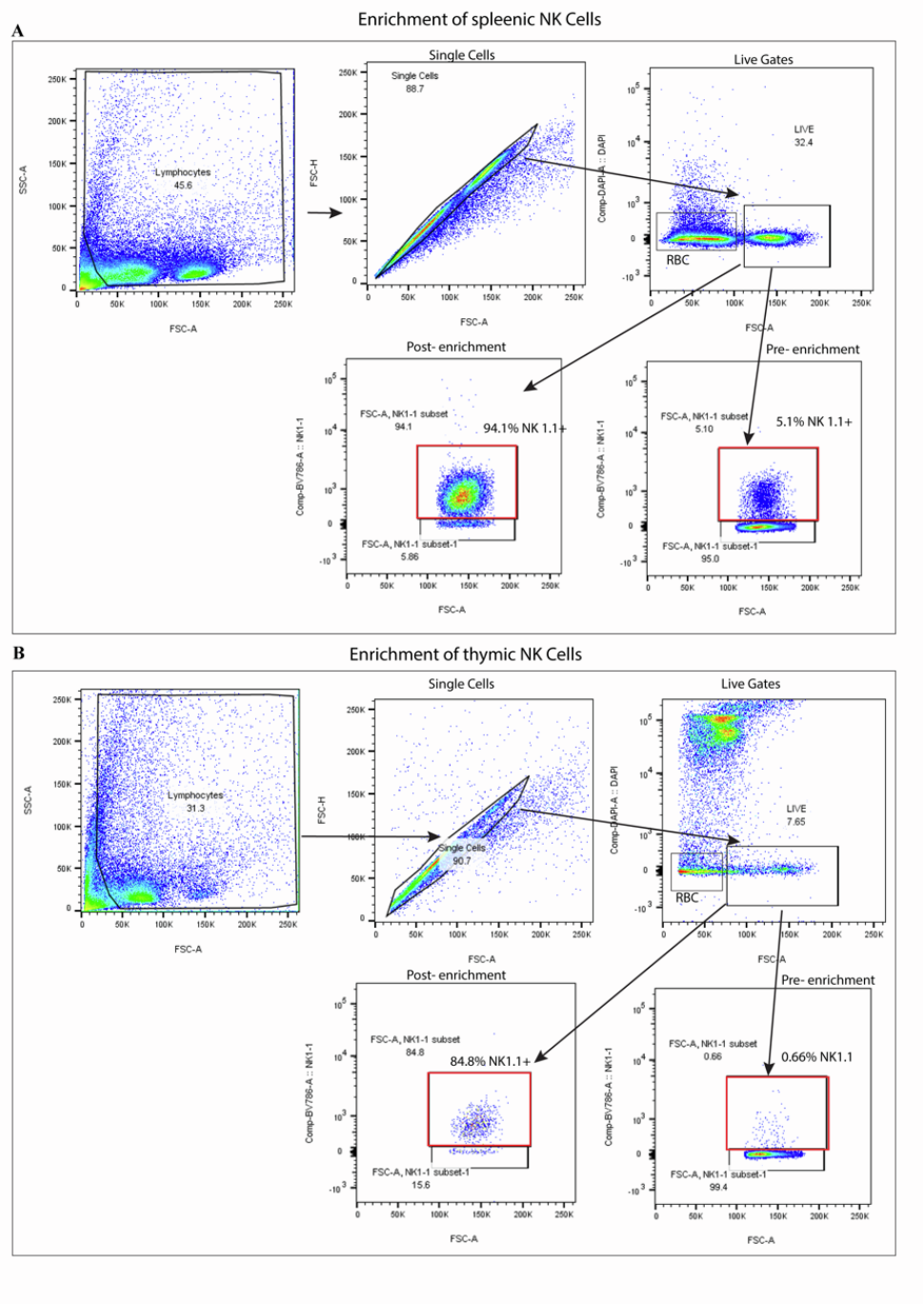

Figure S1. Isolation of untouched NK cells from spleen and thymus by using the NK cell Isolation kit "MojoSort™" by BioLegend. Sample gating strategy for calculating purity of isolated NK cells. After gating on live single cell lymphocytes using forward and side scatter profiles and DAPI dye exclusion, the NK cell percentages were determined using NK 1.1 antibody staining. **A**. High levels of NK cell purity were obtained from spleen tissue (enriched from 5.1% to 94%). **B.** High levels of NK cell purity were obtained from Thymic tissue (enriched from 0.66% to 84.8%). Contaminating cells non-immune.

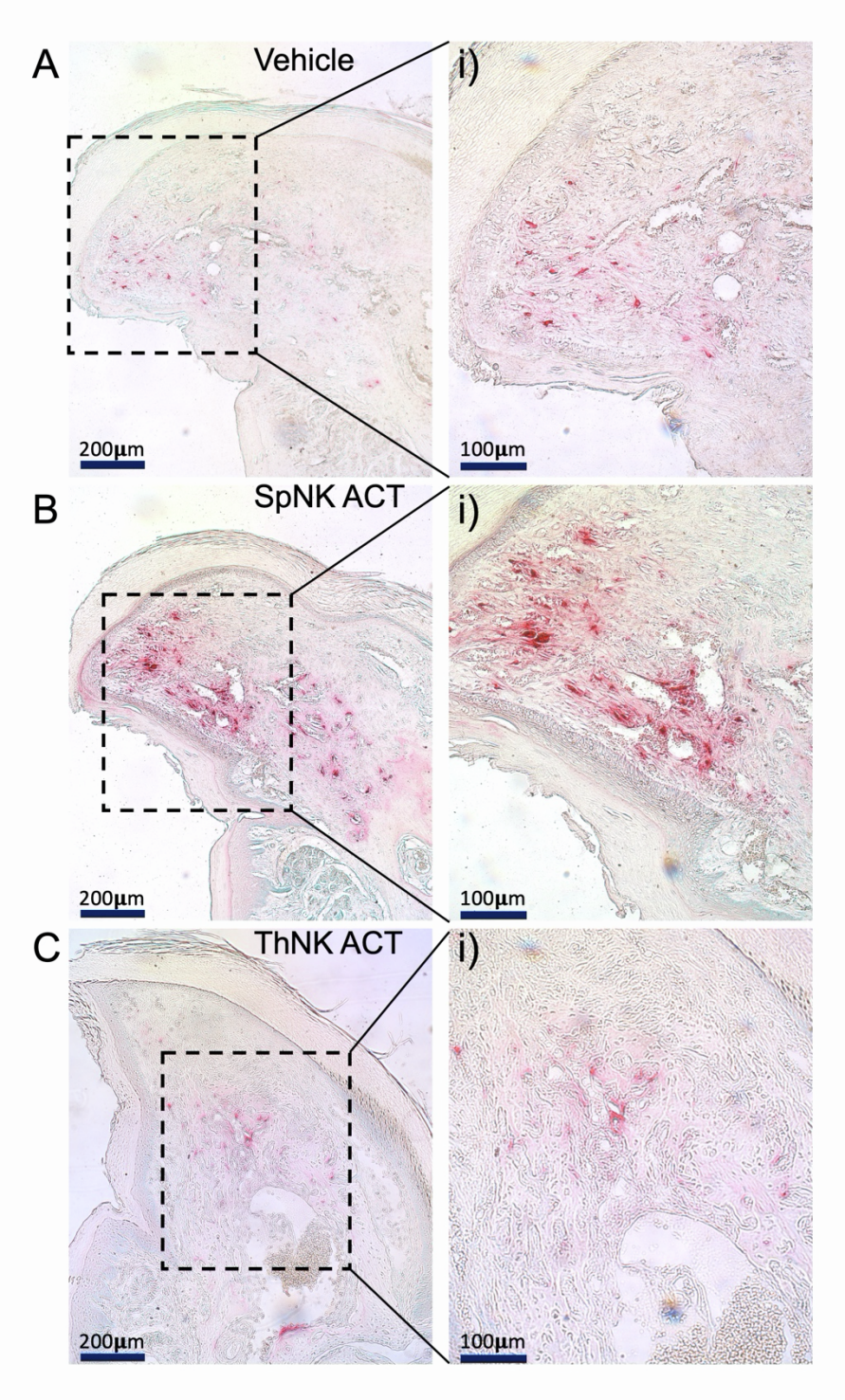

Figure S2. ***ThNK ACT into NSG mice causes a reduction in the number of osteoclasts at 12DPA compared to vehicle treated animals where SpNK ACT causes osteoclast induction.***
Representative TRAP+ osteoclast staining on paraffin embedded sections. Images taken at 10x and 20x. Scale bar as shown.

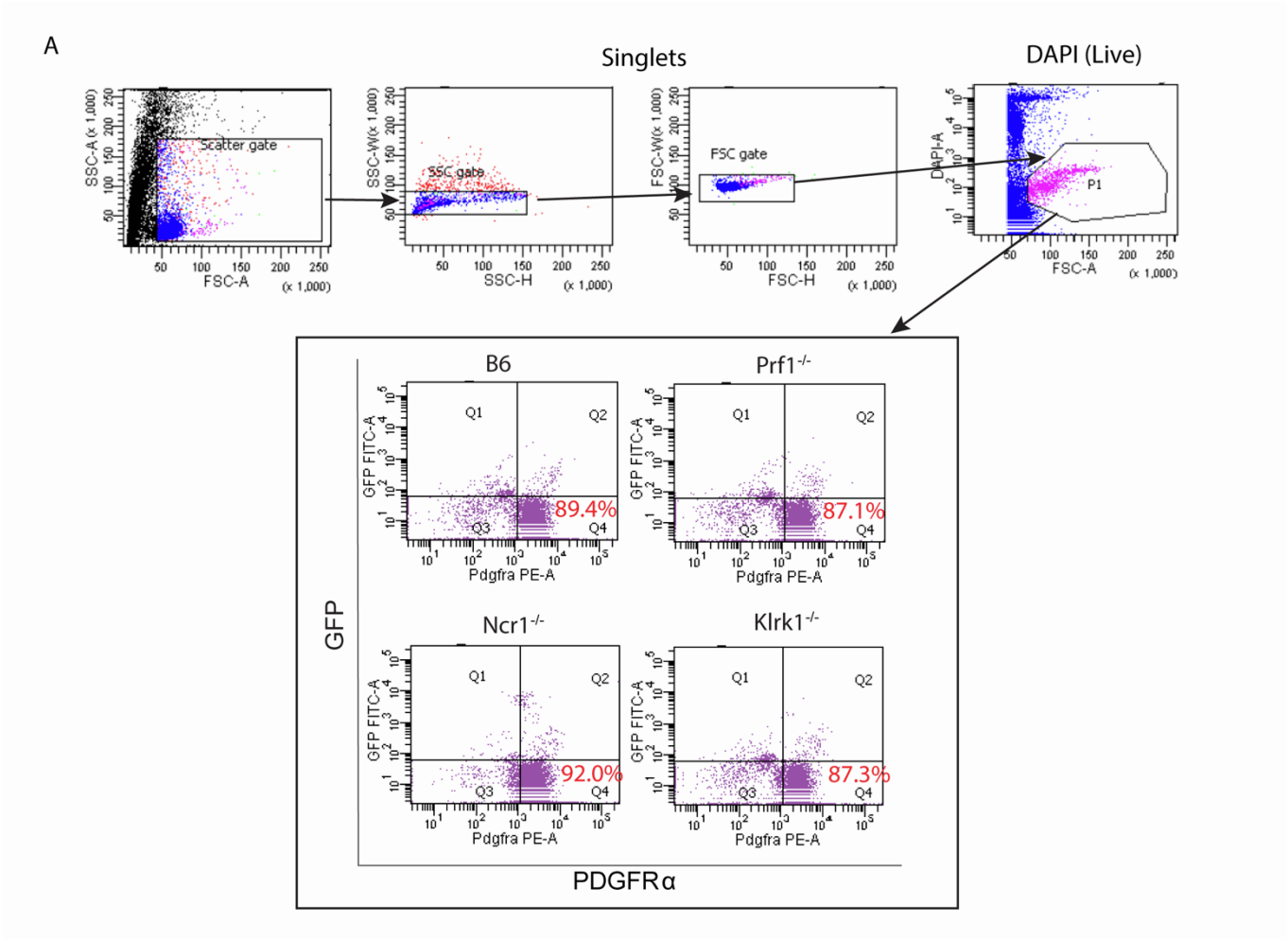

Figure S3. Fluorescence-activated cell sorting (FACS) -BD FACSymphony™ S6- was used to sort for PDFGRα positive cells. Single cells were identified by plotting forward side scatter-area- vs forward scatter-height. Single cells were then separated from dead cells by DAPI. *PDGFRα*$^{+}$ positive cells from B6, Prf$^{-/-}$, Ncr 1$^{gfp/gfp}$ and Klrk $^{-/-}$ were sorted before use in autologous NK cytotoxicity assays. Sorting was performed on 20 pooled digits per genotype (N=5 mice) and purified cells used in cytotoxicity assays.